Proceedings of the 28th IEEE
EMBS Annual International Conference
New York City, USA, Aug 30-Sept 3, 2006

Cavity-Enhanced Biosensing Utilizing Plasmon Resonance Modes

D. Razansky[1], P. D. Einziger[2], and D. R. Adam[1]
Departments of Biomedical[1] and Electrical[2] Engineering, Technion – Israel Institute of Technology, Haifa, Israel
Electronic mail: danir@tx.technion.ac.il

Abstract **– Traditionally, surface plasmon resonance (SPR) biosensors utilize absorption of light radiation incident upon noble metal films above the total internal reflection angles. Herein we extend the SPR phenomenon to incorporate cavity plasmon resonance (CPR) excitation of metallic films at incidence angles below the critical angle. While SPR occurs for TM polarized light only and requires very specific excitation conditions, which could be disadvantageous in some practical designs, CPR does not require complicated evanescent field excitation above the critical total internal reflection angle and can be implemented for both transverse electric (TE) and transverse magnetic (TM) fields even under normal incidence (TEM). These and other unique features of CPR enable a more flexible design of highly efficient and sensitive biosensing devices.**

Introduction

Surface plasmon resonance (SPR) is known as one of the most sensitive subwavelength biosensing microscopy, spectroscopy and imaging methods for characterization of surface physical properties of materials and adsorbates (e.g. [1]-[6]). In the most common geometrical setup (the Kretschmann configuration depicted in Fig. 1(a)), an electromagnetic (EM) radiation from the visible or near-infrared spectrum is incident above the total internal angle upon thin metallic film, located between a high refractive index prism and an analyte under investigation. Maximal sensitivity is achieved whenever film thickness is optimally selected as to allow for the full absorption conditions. An important property of surface plasmons is the EM field enhancement at the interface compared with the incoming radiation. This enhancement can reach a factor of about 10 for a smooth flat surface and even more for a rough surface [7], and suggest s using surface plasmons for surface-enhanced spectroscopy, like the surface plasmon fluorescent spectroscopy. The fields associated with the surface plasmons extend into the media adjacent to the interface and exponentially decaying away from it. Being limited to near-plasma frequencies of metals, lying in the visible and near-infrared bands, surface plasmons can be excited under very specific conditions and usually have poor penetration depth into adsorbing layers. The resulting device is capable of measuring the refraction index of very thin layers of material adsorbed on a metal.

Herein we suggest an alternative method of plasmon resonance excitation by utilizing cavity plasmon resonance (CPR) phenomenon. Devices using CPR instead of SPR do not require complicated evanescent field excitation above the critical total internal reflection angle and can be implemented for both transverse electric (TE) and transverse magnetic (TM) fields even under normal incidence (TEM), thus offering more flexibility over wide ranges of wavelengths, bandwidths, and device dimensions.

Prototype configurations

The two prototype configurations under consideration are depicted in Fig. 1. The SPR configuration (Fig. 1(a)) consists of a thin metallic film of thickness d with generally complex permittivity ε_2, which is asymmetrically surrounded by two semi-infinite layers, having the corresponding constants ε_1 and ε_3, all assumed to be linear and isotropic. For the CPR configuration (Fig. 1(b)), a perfect mirror is placed at a distance ℓ from the metallic film.

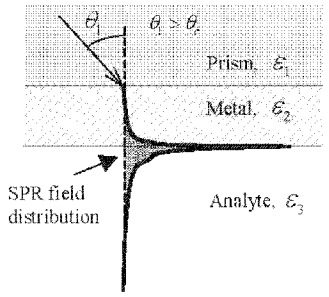

(a) SPR-supporting configuration

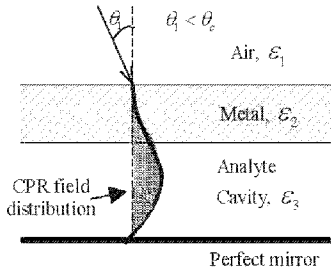

(b) CPR-supporting configuration

Fig. 1. Biosensing configurations utilizing absorbing metallic film.

Assuming a harmonic time dependence $e^{-i\omega t}$ of the obliquely incident plane wave, the corresponding wave numbers $k_1=\omega\sqrt{\varepsilon_1\mu_0}$, $k_2=\omega\sqrt{\varepsilon_2\mu_0}$, and $k_3=\omega\sqrt{\varepsilon_3\mu_0}$ satisfy $\Im\{k_1\},\Im\{k_2\},\Im\{k_3\}\geq 0$, respectively. As shown in Fig. 1, the electromagnetic wave is incoming through the upper layer k_1 and impinges upon the absorbing film k_2 at some angle θ_1. As usual, the propagation angles in all the layers are determined via Snell's law, i.e. $k_1\sin\theta_1=k_2\sin\theta_2=k_3\sin\theta_3$. Subsequently, the critical incidence angle θ_c is given via $\theta_c=\sin^{-1}(k_3/k_1)$. For either total internal reflection configuration (Fig. 1(a)) or perfect mirror configuration (Fig. 1 (b)) the power absorption efficiency is given via

$$\eta=1-|R|^2, \tag{1}$$

which is a direct extension of the formulation developed in [8] and [9] for the current case of zero power transmitted through the film. The global reflection coefficient R can be conveniently expressed via

$$R=\frac{r_1+\rho_2 e^{2ik_2 d\cos\theta_2}}{1+r_1\rho_2 e^{2ik_2 d\cos\theta_2}}, \tag{2}$$

where the local refraction coefficients r_1 and ρ_2 are defined via

$$r_1=\frac{1-\mathcal{Z}_{12}}{1+\mathcal{Z}_{12}},\quad \rho_2=\frac{\mathcal{Z}_{12}-\tilde{\mathcal{Z}}_{13}}{\mathcal{Z}_{12}+\tilde{\mathcal{Z}}_{13}},\quad \mathcal{Z}_{lq}^{\frac{TE}{TM}}=\frac{k_q}{k_l}\left(\frac{\cos\theta_q}{\cos\theta_l}\right)^{\pm 1}. \tag{3}$$

The normalized impedance $\tilde{\mathcal{Z}}_{13}$ is defined via

$$\tilde{\mathcal{Z}}_{13}=\begin{cases} i\mathcal{Z}_{13}\cot(k_3\ell\cos\theta_3), & Fig.1(b)\\ \mathcal{Z}_{13}, & Fig.1(a)\end{cases}. \tag{4}$$

The distinguishing superscripts TE and TM, corresponding to the two elementary plane-wave polarizations, have been partially omitted in Eqs. (1)-(4), only for relations applying to both polarizations. This rule is adapted throughout the paper for all the equations that apply to both polarizations.

Optimal Absorption Paths and Material Dispersions

The actual biosensing procedure, i.e. measurement of physical parameters (e.g. refractive index) of the analyte layer ε_3, can be optimally facilitated by founding the conditions of total absorption of the incident radiation in the metallic film, leading to $\eta=1$ or $R=0$ in (1).

To clarify the current analytical formulation, we obtain explicit asymptotic expressions for the optimal absorbing film material as a function of its various parameters (normalized thickness $k_1 d$, distance from the substrate $k_3\ell$, angle of incidence θ_1). Two asymptotic full absorption cases are of particular interest, namely, the limit of a thin layer, i.e. $k_1 d<<1$, and the limit for which the absorbing film cannot be considered as thin, i.e. $k_1 d\sim 1$. Following the procedures described in [8], while requiring $R=0$ in (2), one obtains asymptotic expressions for the optimal film impedance $\mathcal{Z}_{12,opt}$ as

$$\mathcal{Z}_{12,opt}=(1+i)\sqrt{\left(1-\tilde{\mathcal{Z}}_{13}\right)/(2\delta)} \tag{5}$$

and

$$\mathcal{Z}_{12,opt}=-\tilde{\mathcal{Z}}_{13}\left(1+2e^{-2\delta\tilde{\mathcal{Z}}_{13}-2/\tilde{\mathcal{Z}}_{13}}\right) \tag{6}$$

in the $k_1 d<<1$ and $k_1 d\sim 1$ limits, respectively, where

$$\delta^{\frac{TE}{TM}}=k_1 d\cos^{\pm 1}\theta_1. \tag{7}$$

Because the focus here is on metallic-type absorbing films, only the zero-order mode ($m=0$ in [8]) optimal asymptotic solution is provided here for the thin-layer limit. Higher-order modes that provide appropriate optimal solutions supported by low loss (insulating) materials are not shown. Note that for the plasmon resonance condition, i.e. $\Im\{\tilde{\mathcal{Z}}_{13}\}<0$, Eqs. (5)-(6) equally hold for both TE and TM polarizations in the CPR case, whereas SPR is possible for TM polarization only.

In the thin film limit ($k_1 d<<1$), the optimally absorbing film material, represented by $\mathcal{Z}_{12,opt}$, is highly dependent on the normalized distance of the substrate layer $k_3\ell\cos\theta_3$. For $p\pi\leq k_3\ell\cos\theta_3<\pi/2+p\pi$, $p=0,1,2,\ldots$, the loss angle of $\mathcal{Z}_{12,opt}$ will be less than 45°, representing low loss materials with $\Re\{\mathcal{Z}_{12}\}>>\Im\{\mathcal{Z}_{12}\}$. When $k_3\ell\cos\theta_3=\pi/2+p\pi$, the loss angle of materials obeys the dispersion condition of good electric conductors, which corresponds to a loss angle of 45° (i.e., $\Re\{\mathcal{Z}_{12,opt}\}=\Im\{\mathcal{Z}_{12,opt}\}$). However, lossy resonance excitation of materials in their conducting state with $k_3\ell\cos\theta_3=\pi/2+p\pi$ is usually not possible for infrared wavelengths and below. The reason is that, as wavelength decreases, the dispersion of good conductors changes its behavior either into metallic-plasma-like or anomalous absorption states whose loss angle deviates from the optimal 45°, thus making the optimal ($\eta=1$) excitation impossible. On the other hand, lossy resonance excitation is indeed possible also at much lower wavelengths by using metals in their near-plasma band. One notes from (4)-(5) that for thin film limit, if $\pi/2+p\pi<k_3\ell\cos\theta_3<(p+1)\pi$, the optimal film is actually of a plasma type since its loss angle is then above 45° since $\Im\{\tilde{\mathcal{Z}}_{13}\}<0$. Moreover, when the film becomes relatively thick (Eq. (6), $k_1 d\sim 1$), the asymptotic optimal solutions are inherently of the plasmon resonance type. Their dispersion is that of metals in their plasma band with loss angle between 45° and 90°.

Table I. Configuration parameters and intersection points for Figs. 2 and 3.

Case #	1	2	3	4	5	6
Absorption Mode	CPR	CPR	CPR	CPR	SPR	SPR
Film material	Al	Ag	Al	Au	Ag	Ag
Film thickness	$k_1 d \approx 1$	$k_1 d \approx 1$	$k_1 d << 1$	$k_1 d \approx 1$	$k_1 d \approx 1$	$k_1 d << 1$
θ_c [°]	-	-	-	-	49.5	49.5
θ_1 [°]	0	0	0	0	51	51
ℓ [μm]	0.043	0.202	0.409	0.389	∞	∞
d_{opt} [nm]	36.44	31.94	5.47	47.04	27	4
λ_{opt} [μm]	0.114	0.463	0.928	0.833	0.510	6.687

The above conclusions are further demonstrated via Fig. 2 where the exact solutions of $R = 0$ for either CPR (Fig. 1(b), setting $\theta_1 = 0$) or SPR (Fig. 1(c)) are represented via optimal absorption paths [8], [9] in the complex $\mathcal{Z}_{12}$ domain. Along each path the value of δ varies continuously whereas the power absorption efficiency η in (1) is exactly 100% for constant $k_3\ell$ and θ_1. It should be noted that the same path is obtained for either CPR or SPR, by properly setting $k_3\ell$ and θ_1 for obtaining identical $\mathcal{Z}_{12}$ in (4).

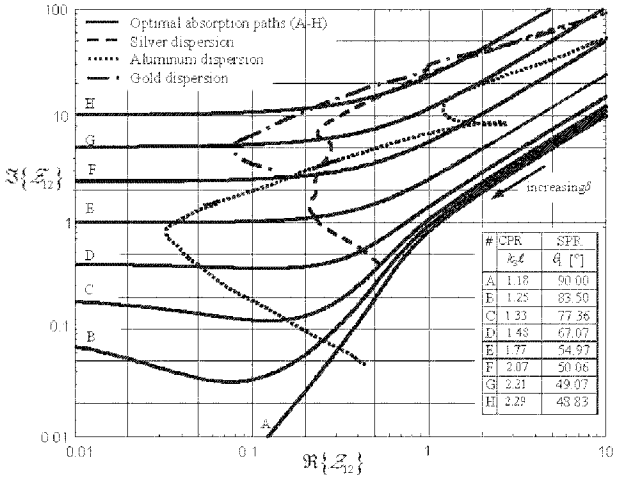

Fig. 2. Optimal absorption paths for various total absorption cases along with some material dispersions [10] in the complex $\mathcal{Z}_{12}$ domain. For the CPR configuration $\theta_1 = 0$ while for the SPR configuration $\Re\{\mathcal{Z}_{13}\} = 0$, $k_3/k_1 = 0.752$, and $\theta_1 > \theta_c = \sin^{-1}(k_3/k_1) = 48.754°$. The analyte layer is represented by water permeability at visible and infrared wavelengths ($\varepsilon_3 = 1.7689$)

Also, normalized dispersions of some noble metal materials (Table I) are depicted in Fig. 2 (dashed lines) versus excitation frequency. The intersection points between the optimal absorption paths and material dispersion curves of the specific metal used represent the full absorption or lossy resonance conditions and provide the required optimal design values, i.e. film thickness d_{opt} and excitation frequency ω_{opt}, per given substrate distance ℓ or incidence angle θ_1.

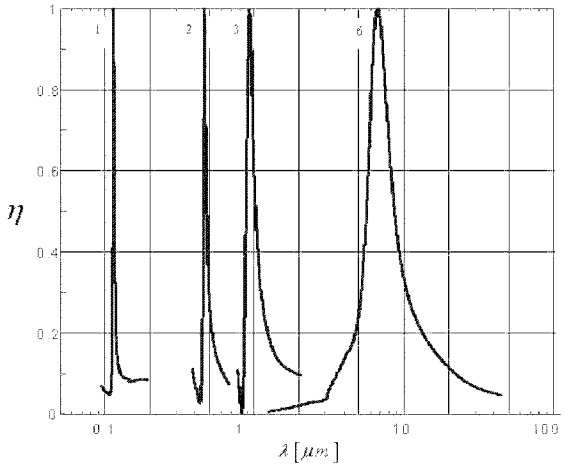

(a)

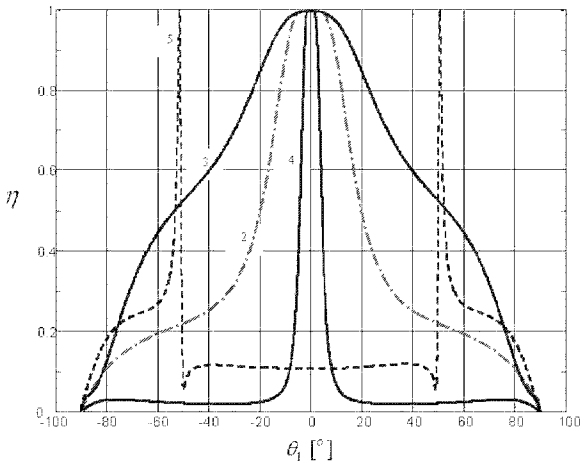

(b)

Fig. 3. Power absorption efficiency in the vicinity of various lossy resonances (configuration details are given in Table I and material dispersions are taken from [10]). (a) dependence versus excitation wavelength $\lambda = c/f$; (b) dependence versus angle of incidence θ_1.

Frequency and Angular Sensitivity

The sensitivity of the power absorption efficiency in the vicinity of different lossy resonance conditions (intersections in Fig. 2) as a function of excitation frequency and incidence angle is shown in Fig. 3, subject to precise configuration parameters given in Table I. The specific examples include CPR and SPR excited silver film in the visible band and excitation of gold and aluminum films in near-infrared and ultraviolet bands. Evidently, the CPR and SPR absorption is inherently characterized by high frequency and/or spatial selectivity. It should be noted however that the CPR excitation offers more flexibility over wide ranges of wavelengths, bandwidths, and device dimensions as can be verified via Table I.

Obviously, the cases shown in Fig. 3 are not the only possible examples and, as suggested by Fig. 2, many other intersection points exist, offering more flexibility for achieving full absorption in thin films over wide range of wavelengths, bandwidths, and device dimensions.

Summary and Conclusion

A new type of plasmon resonance excitation in thin metallic films, utilizing the cavity plasmon resonance phenomenon, was proposed. Analytic derivation rendered closed-form formulae for characterization of optimal material (metal) dispersion assuring full absorption (no reflection) conditions in both CPR and SPR configurations. The performance of various CPR configurations was compared to this of the SPR in both frequency and angular domains. The results of the current feasibility study suggest that CPR holds a great promise of becoming a very robust and flexible biosensing technique for ultrasensitive refractive index measurements.

References

[1] E. A. Smith and R. M. Corn, "Surface plasmon resonance imaging as a tool to monitor biomolecular interactions in an array based format", *Appl. Spectr.*, 57(11), pp. 320A-332A, 2003.

[2] M. Specht, J. D. Pedarnig, W. M. Heckl, and T. W. Hänsch, "Scanning plasmon near-field microscope", *Phys. Rev. Lett.*, 68, pp. 476-479, 1992.

[3] I. I. Smolyaninov, J. Elliott, A. V. Zayats, and C. C. Davis, "Far-field optical microscopy with a nanometer-scale resolution based on the in-plane image magnification by the surface plasmon polaritons", *Phys. Rev. Lett.*, 94, 057401, 2005.

[4] S. Maruo, O. Nakamura, and S. Kawata, "Evanescent-wave holography by use of surface-plasmon resonance", *Appl. Opt.*, 36(11), pp. 2343-2346, 1997.

[5] B. P. Nelson, A. G. Frutos, J. M. Brockman, and R. M. Corn, "Near-infrared surface plasmon resonance measurements of ultrathin films. 1. Angle shift and SPR imaging experiments", *Anal. Chem.*, 71(18), pp. 3928-3934, 1999.

[6] I. R. Hooper and J. R. Sambles, "Sensing using differential surface plasmon ellipsometry", *J. Appl. Phys.*, 96(5), pp. 3004-3011, 2004.

[7] H. Raether, *Surface Plasmons on Smooth and Rough Surfaces and on Gratings*, Springer, Berlin, 1988.

[8] D. Razansky, P. D. Einziger, and D. R. Adam, "Optimal dispersion relations for enhanced electromagnetic power deposition in dissipative slabs", *Phys. Rev. Lett.*, 93(8), 083902, Aug. 2004.

[9] D. Razansky, P. D. Einziger, and D. R. Adam, "Optimization of bulk and surface biosensing in plane stratified configurations", *Proc. 27th Ann. IEEE Eng. Med. Biol. Soc. Int. Conf.*, Shanghai, China, Sep. 2005.

[10] M. J. Weber (editor), *Handbook of Optical Materials*, CRC Press, 2003.